Res Chem Intermed
DOI 10.1007/s11164-012-0839-8

Electrochemical properties of PEO/PMMA blend-based polymer electrolytes using imidazolium salt-supported silica as a filler

Lyungyu Lee · Ick-Jun Kim · Sunhye Yang · Seok Kim

Received: 7 August 2012 / Accepted: 26 September 2012

Abstract In this study, the composite polymer electrolytes (CPEs) were prepared by solution casting technique. The CPEs consisted of PEO/PMMA blend as a host matrix doped with $LiClO_4$. Propylene carbonate (PC) was used as plasticizer and a small amount of imidazolium salt-supported amorphous silica (IS-AS) as a filler was prepared by the sol–gel method. At room temperature, the highest conductivity was obtained for the composition having PEO–PMMA–$LiClO_4$–PC–4wt. % IS-AS with a value of 1.15×10^{-4} S/cm. In particular, the CPE using the IS-AS filler showed a higher conductivity than any other sample (fumed silica, amorphous silica). Studies of differential scanning calorimetry and scanning electron microscopy indicated that the ionic conductivity increase was due to an expansion in the amorphous phase which enhances the flexibility of polymeric chains and the homogeneous structure of CPEs. It was found that the ionic conductivity and interfacial resistance stability of CPEs was significantly improved by the addition of IS-AS. In other words, the resistance stability and maximum ambient ionic conductivity of CPEs containing IS-AS filler were better than CPEs containing any other filler.

Keywords Composite polymer electrolyte · PEO · PMMA · Imidazolium salt-supported amorphous silica · Ionic conductivity

---

L. Lee · S. Kim (✉)
Department of Chemical and Biochemical Engineering, Pusan National University, San 30, Jangjeon-dong, Geumjeong-gu, Busan 609-735, South Korea
e-mail: seokkim@pusan.ac.kr

I.-J. Kim · S. Yang
Battery Research Group, Korea Electrotechnology Research Institute, 28-1, Seongju-dong, Changwon 641-120, South Korea

Introduction

Lithium ion batteries are overwhelmingly used for various applications and the usage is expected to expand in the future. However, the severe reactivity of lithium metal on the electrodes greatly limits the choice of usable electrolytes and incurs safety problems with the commercialization of rechargeable batteries. Because solid state electrolytes are in demand for use in high-capacity Li batteries, an ideal way to obtain a light-weight, leak-proof and flexible lithium ion battery is to utilize solid polymer as an electrolyte [1–5].

Organic solid electrolytes, as well as inorganic ones, have been widely studied, and polymeric solid electrolytes are especially expected to be excellent composites because of their flexibility and processibility. Since the ionic conductivity of the PEO/LiX complex was measured in 1973 [6], extensive research and development has been done on solid polymer electrolytes (SPEs) during the past three decades. Recently, SPEs containing dissolved metal salts have been proposed as an alternative to a liquid electrolyte in rechargeable lithium batteries. The advantages of SPEs are their capability for high-speed production of thin bipolar cells and enhanced safety due to the absence of liquid electrolytes. This has promoted the development of dry, gelled, and porous types of SPEs [7, 8]. PEO is one of the most promising SPEs. However, due to the poor ionic conductivity ($\sigma = 10^{-8}$–10^{-7} S/cm) of these polymer electrolytes at an ambient operating temperature, various modifications have been carried out [9].

Blending of different polymers provides easy preparation and control of the physical properties within the miscibility compositional region, and the blends often exhibit properties that are superior to the properties of individual components of the blend [10, 11]. Since the polymer blending technique can offer versatile and useful routes for improving polymeric material properties, it has been employed and applied for many polymeric systems [12]. A broad range of studies on miscibility [13, 14], crystallization [15, 16], structure [17], and dynamics [18] for poly(ethylene oxide) methyl(PEO)/poly(methyl methacrylate) (PMMA) systems have been investigated. PEO/PMMA blends have been reported as marginally miscible [19] with a weak enthalpic interaction, i.e., $\chi_{12} \cong 0$ [20], implying that they can often be immiscible in certain temperature and composition ranges. The miscibility of this blend is strongly dependent on the tacticity of PMMA [21].

Many kinds of ceramic fillers, such as Al_2O_3 [22–24], ZnO [25, 26], TiO_2 [27], ZrO_2 [28], SiO_2 [29–31] etc., layered clays, e.g., montmorillonite [32–34], and organic–inorganic hybrid materials [35–37] have been used as a second phase for polymer electrolytes to obtain composite polymer electrolytes (CPEs). The addition of an inert ceramic filler has proved an effective approach to improve the overall performances of polymer electrolytes, which usually showed improved mechanical performances and even enhanced ionic conductivity and interface stability with various electrode materials [38–40].

Ionic liquids (ILs) have been attracting much attention in view of their potential applications as new types of electrolytes in many electrochemical devices. This continuously growing interest is motivated by their unique properties such as nonvolatility, nonflammability, negligible vapor pressure, high ionic conductivity, broad electrochemical window, and special characteristics in comparison with conventional organic and inorganic solvents [41–43]. In the past decade, there has been increasing use of ILs containing imidazolium and its counter anions in many research fields such as Li batteries [44], dye-sensitized solar cells [45], separation science, and material synthesis [46].

In this study, imidazolium salt-supported amorphous silica (IS-AS) was prepared by the sol–gel method as described previously [47]. The as-prepared IS-AS was used as a filler to prepare a series of PEO/PMMA blend-based CPEs with $LiClO_4$. It was anticipated that the mesoporous structures of IS-AS and the amorphous PEO/PMMA matrix would provide shorter ion transport paths, resulting in higher conductivity and better electrochemical stability. Therefore, the effects of the addition of IS-AS on the micro-structure and electrochemical property of the CPEs were studied.

Experimental

Materials

Poly(ethylene oxide) and poly(methyl methacrylate) with average molecular weights of 10^6 (Aldrich) and 1.2×10^5 (Aldrich), respectively, were used without further purification. Lithium perchlorate ($LiClO_4$) was obtained from (Aldrich) and was dried under vacuum ($<10^{-3}$ Torr) for 24 h at 80 °C before use. Acetonitrile (ACN) and propylene carbonate (PC) were acquired from Junsei (Japan), and used without further purification. The IS-AS was prepared according to the method reported previously by Ref. [47]. Amorphous silica and fumed silica as fillers to compare with IS-AS were acquired from Kanto (35 μm) and Aldrich (7 nm), respectively, and used without further purification.

Preparation of IS-AS (Imidazolium salt supported amorphous silica)

Imidazole (5.1 g, 79.5 mmol) was dissolved in 75 mL of dry toluene, to which 3-chloropropyltriethoxysilane (ClPTES, 18 mL, 75 mmol) was added, and the mixture was refluxed for 12 h under an argon atmosphere. An oil containing 3-(*N*-imidazolyl)propyl triethoxysilane was obtained, and to it was added 1-bromobutane, followed by refluxing for another 12 h under argon to yield 1-(triethoxysilylpropyl)-3-*n*-butylimidazolium bromide. This is denoted as IL-functionalized organosilane (IFOS). The molar ratio of the constituents of the synthetic mixture was optimized according to a previous report [48]; $0.818TEOS:0.182IFOS:5.61HCl:153.9H_2O$, where the ratio of tetraethyl orthosilicate (TEOS) to IFOS was 4.5. In a typical synthesis, a 500-mL polypropylene (PP) bottle, fitted with a wheel-type magnetic bar and brought to 40 °C, was charged with 100 mL of water, followed by 25 mL of 35 % HCl. After 15 min of stirring, a clear solution was obtained. Before 8.01 mL of TEOS was added, it was placed in the open PP bottle and stirred for 3 h at 40 °C for prehydrolysis and expulsion of ethanol from the reaction mixture. Then, 4.64 mL of the IFOS–ethanol mixture was added (initial organosilane mixed with 15 mL of ethanol to avoid errors in the measurement of the more viscous IFOS) into the aforementioned solution and stirred for 24 h at 40 °C; it was subsequently heated for another 24 h at 60 °C in a hot-air oven in the PP bottle. The solid product was recovered and mixed with 50 mL of ethanol, filtered, and dried at 60 °C for 12 h.

Preparation of composite polymer electrolytes

All the CPEs were prepared using the solution casting technique. The CPEs system entailed the use of PEO and PMMA blend polymer matrix in a molar ratio of 4:1, PEO and $LiClO_4$ salt in a molar ratio [EO]:[Li] of 16:1, and PEO and PC plasticizer in a molar ratio 1:0.1, with a different weight ratio IS-AS. The preparation of CPE films involved first the dissolution of PEO, PMMA and PC in ACN at room temperature for several hours, after which $LiClO_4$, filler was added to the PEO/PMMA/PC polymer matrix solution prepared. After a completely homogenous mixture was obtained, it was cast onto a Petri dish and any residual solvent such as an ACN were evaporated in a dry oven at 60 °C for 24 h. Finally, resultant electrolyte films were obtained. The obtained SPE was peeled from the laboratory dish and stored inside the glove box.

Characterization

Surface area, pore volume, and pore size distribution were measured by nitrogen adsorption at 77 K using a BET apparatus (ASAP 2010; Micromeritics). The solvent-extracted samples were degassed at 110 °C and 10^{-5} Torr overnight before adsorption experiments. The mesoporous volume was estimated from the amount of nitrogen adsorbed at a relative pressure of 0.5 by assuming that all mesopores had been filled with condensed nitrogen in the normal liquid state. The pore size distribution was estimated using the Barrett, Joyner, and Halenda (BJH) algorithm (ASAP 2010) built-in software from Micromeritics. Spectral measurements were recorded between 4,000 and 400 cm^{-1}. ^{29}Si solid-state NMR experiments were carried out at frequencies of 79.5 MHz.

The morphology of the CPE films was investigated by Scanning electron microscopy (SEM) (Hitachi S3500 N). Differential scanning calorimetry (DSC) studies were performed in the 0–100 °C range with a Perkin-Elmer (Pyris 1) system, at a heating rate of 5 °C/min and with purging nitrogen gas.

Measurements of electrochemical properties were carried out using a Iviumstat (IVIUM Technologies, Netherlands). The ionic conductivity measurements of the CPEs were carried out by means of AC impedance spectroscopy over the frequency range from 200 kHz to 10 Hz. The impedance measurements were performed by sandwiching the films between two stainless-steel (SS) electrodes. The conductivity values (σ) were calculated from the bulk resistance (R_b), which was determined by equivalent circuit analysis software.

$$\frac{1}{\sigma} = \frac{R_b A}{t} \tag{1}$$

where R_b is the bulk resistance, and t and A are the thickness of the electrolytes film and the areas of film, respectively.

Results and discussion

Structure of IS-AS (imidazolium salt supported amorphous silica)

Figure 1a shows the solid state ^{29}Si MAS NMR spectra of BMImBr-AS confirmed the presence of organo-functionalized moieties ionically coupled with surface of self-assembled porous silica. Distinct resonances can be clearly observed for the siloxane [Qn = Si(OSi)n(OH)$_{4-\mathrm{n}}$, $n = 2$–4; Q_3 at -121 ppm and Q_4 at -130 ppm] and organosiloxane [Tm = RSI(OSi)m(OH)$_{3-\mathrm{m}}$, $m = 1$–3; T_3 at -86 ppm; T_2 at -76 ppm] units.

Figure 1b shows the morphology of the BMImBr-AS which were characterized by SEM. It shows the presence of spherical particles with a regular shape. To study the pore structure of the IS-AS (BMImBr-AS), the surface and adsorption parameters, including the specific surface area (SBET), the BET's constant (CBET), the total pore volume (VT), and the BJH average pore diameter (DBJH), and an immobilized amount of IL, were measured through the N2 adsorption–desorption isotherm; the data are shown in Table 1. The BET surface area of the BMImBr-AS was 364 m^2/g and the pore diameter was 75.9 Å, and average pore volume was 0.7 cm^3/g. Nitrogen content in the BMImBr-AS was analyzed by elemental analysis, and the immobilized amount of IS was 1.92 mmol/g—SiO2. It seems that the IFOS incorporation onto the silica materials is performed successfully through the template-free route.

Ionic conductivity behaviors of CPEs containing IS-AS

In order to enhance the ionic conductivity, studies of the effects on the ion-conducting behavior of CPEs containing specific amounts of fillers were carried out. As a result, the ionic conductivity increased with increasing IS-AS content, and attained the maximum value, 1.15×10^{-4} S/cm, when the IS-AS content is 4wt. % (inset of Fig. 2a). Subsequently, the ionic conductivity decreases slightly with further increase in IS-AS content over 4wt. %. These decreases in the conductivity were due mainly to the decreased ion mobility, which was related to the micro-structure and morphology of CPE. The decrease of the conductivity for filler concentrations higher than 4wt. % can be caused not only by particles aggregation but also by the dilution effect of introducing a non-conducting phase in a conducting one. From this result, the optimum content of IS-AS filler was decided as 4wt. %.

Figure 2a shows the impedance plots for various filler (amorphous silica, fumed silica) containing CPEs at 25 °C. In the case of no filler, the graph shows a rather large-diameter semicircle. The approximate bulk resistance value can be obtained with reference to the touch point at the x-axis. By contrast, the CPEs containing IS-AS filler showed the smallest diameter semicircles. In other words, the CPEs showing the smallest diameter semicircles demonstrated the most superior electrical conductivity confirmed by the low resistance value.

Figure 2b shows the effect of IS-AS filler on the enhancement of the room temperature ionic conductivity of CPEs. The enhancement of ionic conductivity was found by an addition of fillers and reaches the maximum value of 1.15×10^{-4} S/cm

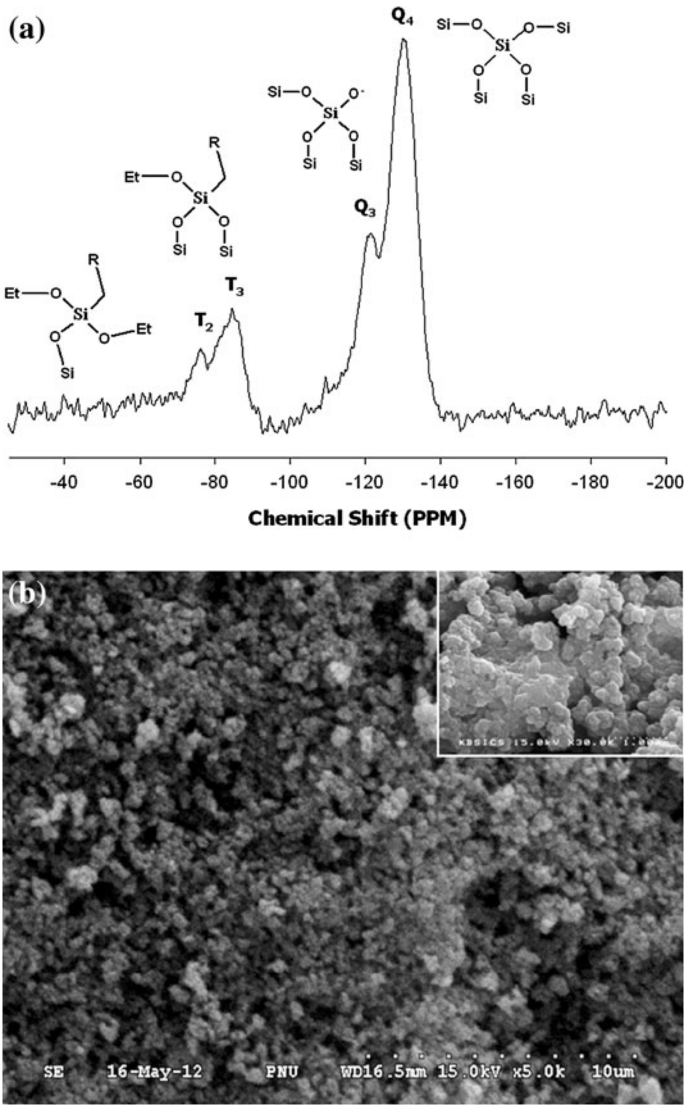

Fig. 1 **a** Si-NMR and **b** SEM images of IS-AS

Table 1 Surface and adsorption parameters of synthesized IS-AS

Sample	ILs content[a] (mmol/g)	S_{BET}[b] (m^2/g)	D_{BJH}[c] (Å)	V_T[d] (m^2/g)
BMImBr-AS	1.92	364	75.9	0.7

[a] Amount of immobilized IL calculated by the nitrogen content of elemental analysis

[b] Specific surface area from BET-method by N_2 adsorption

[c] BJH average pore diameter

[d] Total pore volume

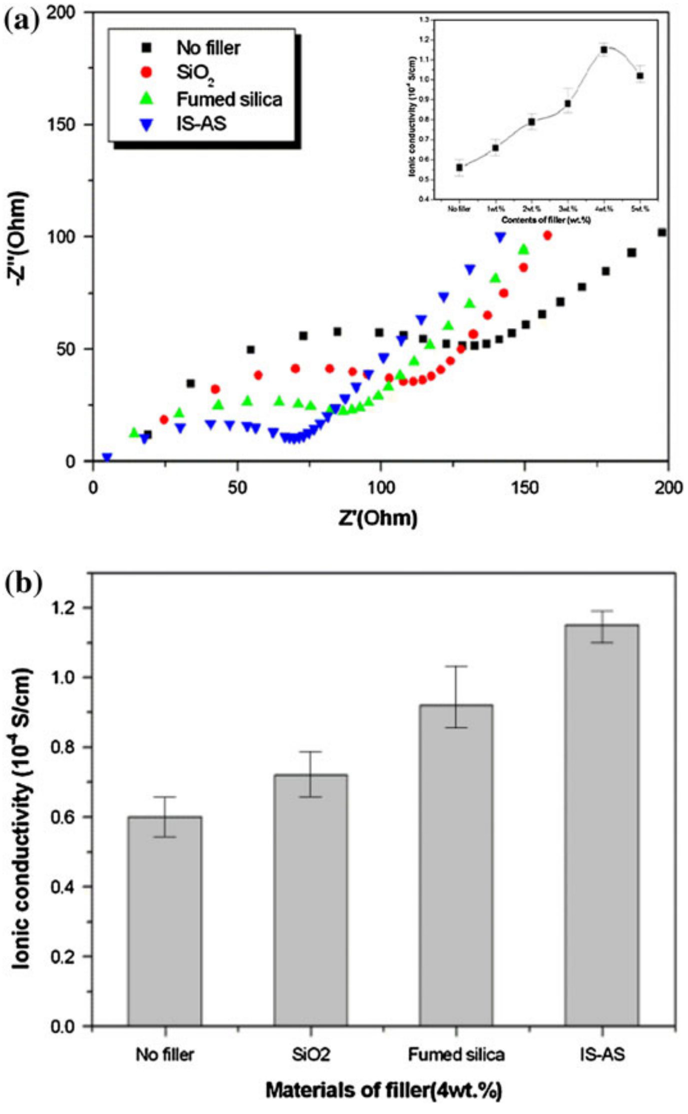

Fig. 2 **a** Impedance plots and **b** ionic conductivity of CPEs with various fillers of equivalent weight contents

at IS-AS filler. This value was double that of the no filler polymer blend (PEO/PMMA) system. This reveals that the charge carriers moved more freely in the CPE with IS-AS than that without IS-AS or other fillers, and this was attributed to the extra interactions between the charge carriers and IS-AS having high surface area, interconnected pores, and high porosity, which provided a more accessible and shorter pathway for transporting the charge carriers. In other words, superior ion behavior and homogeneous particles dispersion of IS-AS filler provided the most suitable environment for the ionic transport and achieved the highest conductivity.

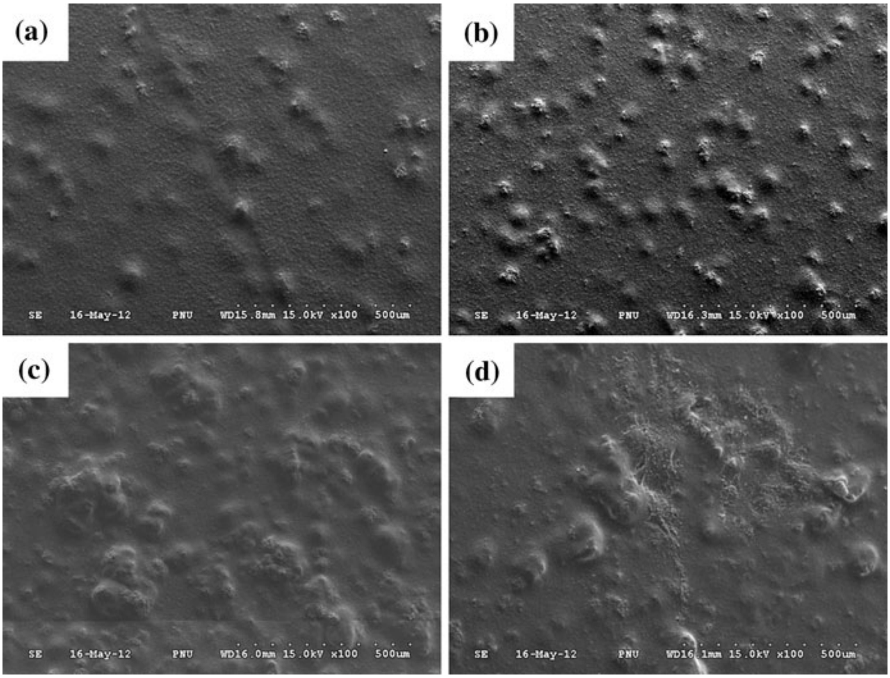

Fig. 3 SEM image of CPEs containing: **a** no filler, **b** amorphous SiO_2, **c** fumed SiO_2, **d** IS-AS

Structural properties of CPEs containing IS-AS

Figure 3 displays SEM images of the CPEs films containing various fillers. In the case of the (a) sample, that is, a pristine film without filler, a rather homogeneous morphology was shown, except for some pores and some white spots probably related to the existence of salt species. By adding various filler content 4wt. %, the film morphology was changed. First of all, at amorphous silica filler, the small phase region had appeared. And, in the case of fumed silica, IS-AS filler, the more homogeneous morphology was shown. Specially, CPEs film morphology containing IS-AS filler appeared, with a wide range of amorphous phase. These phenomena could be explained by improvement of the ion transport ability by miscibility increase between PEO and PMMA polymer chains by uniform particle dispersion of the IS-AS filler. By adding modified filler, the polymer homogeneous feature was developed. Consequently, it can be stated that the presence of the IS-AS filler improved the ionic conductivity of the CPEs. This conductivity could be related to the improvement of the ion transport ability.

Figure 4 shows the DSC results for the pure PEO and CPEs containing various fillers. The melting transitions, corresponding to crystalline to amorphous transition, were shown in DSC data. The endothermic curves began to rise below the melting point. The relative percentage of crystalline (χ_c) has been calculated by referencing pure PEO as 100 % crystalline. It can be calculated with the equation:

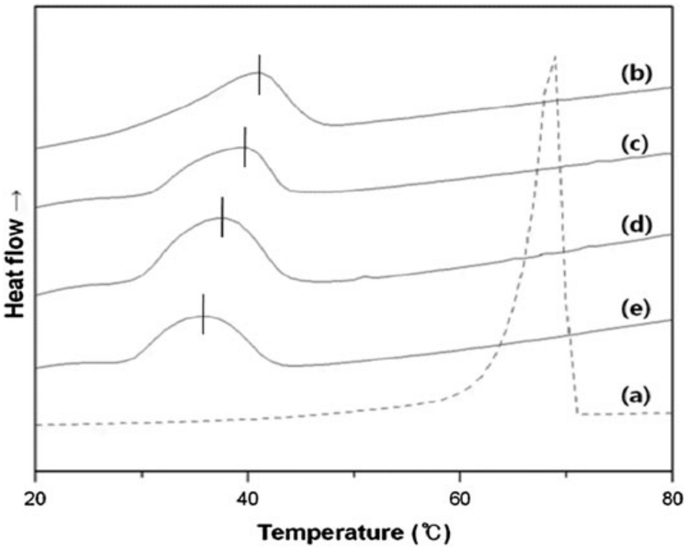

Fig. 4 DSC curves of CPEs containing: *a* pure PEO, *b* no filler, *c* amorphous SiO_2, *d* fumed SiO_2, *e* IS-AS

$$\chi_C = \frac{\Delta H_f}{\Delta H_f^\circ} \tag{2}$$

where ΔH_f° the melting enthalpy of a completely crystalline PEO is the sample and ΔH_f is the experimental enthalpy.

Figure 4 shows the DSC curves for the effect of PEO/PMMA blending and various fillers as an additive in the CPEs. It was found that the PEO showed endothermic peaks due to the melting of the crystalline domain of the PEO with increasing temperature, and the curves moved to a low temperature region by the addition of fillers. It was found that the melting temperature (*T*m) of crystalline PEO was around 35 ~ 42 °C, which was slightly degraded when the filler was added. Also, the crystallinity of CPEs containing IS-AS was decreased the most among the fillers. Consequently, it can be stated that the presence of filler improved the ionic conductivity of the CPEs by slightly decreasing the CPEs crystallinity [49].

DSC studies indicated that the PEO crystallinity was diminished by the addition of filler. The melting temperature, heat of fusion, and relative crystallinity values are listed in Table 2. The PEO itself shows a heat of fusion of 147.8 J/g, and no filler, 32.5 J/g, the estimated crystallinity being 22 %. This indicates that PMMA can reduce the crystallinity of PEO by means of blending effects. With the addition of the IS-AS filler, the *T*m gradually fell to 36.24 °C, and the crystallinity fell to its smallest value, 13 %.

Electrochemical stability of CPEs containing IS-AS

The variation of interfacial impedance of CPEs containing various filler has been analyzed under prolonged exposure at room temperature and is presented in Fig. 5.

Table 2 DSC data for CPEs with various fillers of equivalent weight contents

Code	Sample	Melting temperature *T*m (°C)	Heat of fusion $\triangle H$ (J/g)	Relative crystallinity X_C (%)
1	Pure PEO	68.68	147.8	–
2	No filler	41.17	32.5	22
3	Amorphous SiO_2	40.00	24.2	16
4	Fumed SiO_2	38.00	22.3	15
5	IS-AS	36.24	19.2	13

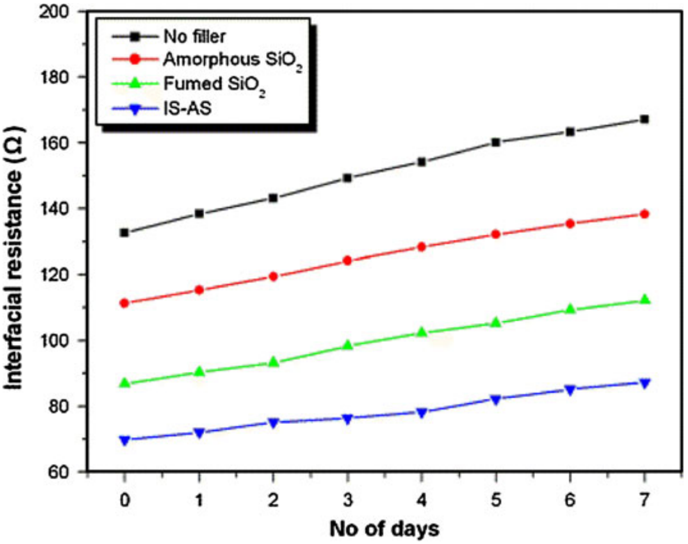

Fig. 5 Variation of interfacial resistance of CPEs with a storage time (SS/CPEs/SS cells, frequency range 200 kHz to 10 Hz, amplitude 10 mV)

It was found that the interfacial resistance of all CPEs increases with storage time. The observed increase in the impedance implies that the electrode was passivated for a long time due to the reactivity between the electrode interfacial and the CPEs. The impedance of CPEs containing filler are smaller than the value of polymer blends without fillers. The composite with IS-AS filler (compared with fumed silica filler) showed better performance than any other samples. The composite with IS-AS not only showed a lower interfacial resistance but also a lower rate of increase in impedance. This can be attributed to the better interfacial stability offered by the modified filler content. In other words, IS-AS filler enabled an improvement in the stability of interfacial resistance and formation of stable SEI layers between electrode and polymer electrolyte.

Conclusions

This study demonstrated that addition of the IS-AS into the PEO/PMMA blend-based polymer electrolyte made the composite a better polymer electrolyte than those without filler. This is related to the fact that the crystalline structure of PEO was weakened due to the possible coordination of Li^+ ions with IS-AS, which was also easily coordinated with the $LiClO_4$ salt.

The addition of IS-AS not only increased the concentration of the solvated Li^+ ions but the interconnected IS-AS filler with high surface area and high porosity also provided a more accessible and shorter pathway, resulting in increasing the mobility of the Li^+ ions in the electrolyte. This phenomenon indicated that the structures of CPEs containing IS-AS filler showed stable morphology, having the larger amorphous phase regions by homogeneous particles dispersion. Furthermore, DSC study had shown the reduced crystallinity values of PEO due to structural deterioration by the addition of PMMA or PC and further by the addition of filler. Especially, with the addition of the IS-AS filler, the Tm and crystallinity values were reduced to the smallest values, 36.24 °C and 13 %, respectively. The ionic conductivity of the PEO/PMMA/IS-AS CPE appeared as the higher ionic conductivity of 1.15×10^{-4} S/cm compared with any other fillers (no filler, amorphous silica, fumed silica). In other words, the CPEs containing IS-AS filler retained the low crystallinity, wide amorphous phase regions, high ionic conductivity, and stable interfacial properties, indicating a possible application in lithium polymer batteries.

Acknowledgments This work was partly supported by the next generation secondary battery R&D program of MKE/KEIT (Grant No. 10042575.2012, Development of 5 kW Zn-air battery for EV and 3.3 V-1,000F pouch type high-power supercapacitor). This research was partly supported by Basic Science Research Program through the National Research Foundation of Korea (NRF) funded by the Ministry of Education, Science and Technology (Grant No.: 2011-0009007).

References

1. F.M. Gray, *Solid Polymer Electrolytes: Fundamental and Technological Application* (VCH, New York, 1991)
2. C.W. Park, Carbon Lett. **12**(3), 180 (2011)
3. F. Croce, G.B. Appetecchi, L. Persi, B. Scrosati, Nature **394**, 456 (1998)
4. M.B. Armand, Annu. Rev. Mater. Sci. **16**, 245 (1986)
5. P.V. Wright, Br. Polym. J. **7**, 319 (1975)
6. D. Fenton, J.M. Parker, P.V. Wright, Polymer **14**, 589 (1973)
7. H.J. Rhoo, H.T. Kim, J.K. Park, T.S. Hwang, Electrochim. Acta **42**, 1571 (1997)
8. S.R. Starkey, R. Frech, Electrochim. Acta **42**, 471 (1997)
9. M. Nookala, B. Kumar, S. Rodrigues, J. Power Sources **111**, 165 (2002)
10. M. Tang, W.R. Liau, Eur. Polym. J. **36**, 2597 (2000)
11. A.M. Rocco, R.P. Pereira, M.I. Felisberti, Polymer **42**, 5199 (2001)
12. J.A. Pathak, R.H. Colby, S.Y. Kamath, S.K. Kumar, R. Stadler, Macromolecules **31**, 8988 (1998)
13. L. Hamon, Y. Grohens, A. Soldera, Y. Holl, Polymer **42**, 9697 (2001)
14. J.C. Machado, G. Coulart Silva, L.S. Soares, J. Polym. Sci. B Polym. Phys. **38**, 1045 (2000)
15. M.S. Lisowski, Q. Liu, J.D. Cho, J. Runt, F. Yeh, B.S. Hsiao, Macromolecules **33**, 4842 (2000)
16. J. Baldrian, M. Horky, A. Sikora, M. Steinhart, P. Vlček, H. Amenitsch et al., Polymer **40**, 439 (1999)
17. S. Schantz, Macromolecules **30**, 1419 (1997)

18. C. Lartigue, A. Guillermo, J.P. Cohen-Addad, J. Polym. Sci. B Polym. Phys **35**, 1095 (1997)
19. J.A. Zawada, C.M. Ylitalo, G.G. Fuller, R.H. Colby, T.E. Long, Macromolecules **25**, 2896 (1992)
20. H. Ito, T.P. Russell, G.D. Wignall, Macromolecules **20**, 2213 (1987)
21. C. Silvestre, S. Cimmino, E. Martuscelli, F.E. Karasz, W.J. MacKnight, Polymer **28**, 1190 (1987)
22. M.A.K.L. Dissanayake, P.A.R.D. Jayathilaka, R.S.P. Bokalawala, I. Albinsson, B.E. Mellander, J. Power Sources **119–121**, 409 (2003)
23. K.M. Bae, B.J. Kim, S.J. Park, Carbon Lett. **12**(3), 121 (2011)
24. X.M. Qian, N.Y. Gu, Z.L. Cheng, X.R. Yang, E.K. Wang, S.J. Dong, Electrochim. Acta **46**, 1829 (2001)
25. H.M. Xiong, X. Zhao, J.S. Chen, J. Phys. Chem. B **105**, 10169 (2001)
26. Z.M. Dang, L.Z. Fan, S.J. Zhao, C.W. Nan, Mater. Res. Bull. **38**, 499 (2003)
27. Y. Liu, J.Y. Lee, L. Hong, J. Appl. Polym. Sci. **89**, 2815 (2003)
28. J.Y. Xi, X.Z. Tang, Chem. Phys. Lett. **393**, 271 (2004)
29. L.Z. Fan, C.W. Nan, S.J. Zhao, Solid State Ion. **164**, 81 (2003)
30. J.W. Kim, K.S. Ji, J.P. Lee, J.W. Park, J. Power Sources **119–121**, 415 (2003)
31. S. Zhang, J.Y. Lee, L. Hong, J. Power Sources **126**, 125 (2004)
32. R.A. Vaia, S. Vasudevan, W. Krawiec, L.G. Scanlon, E.P. Giannelis, Adv. Mater. **7**, 154 (1995)
33. L.Z. Fan, C.W. Nan, M. Li, Chem. Phys. Lett. **369**, 698 (2003)
34. S. Kim, S.J. Park, J. Colloid Interface Sci. **332**, 145 (2009)
35. H.M. Kao, C.L. Chen, Angew. Chem. Int. Ed. **43**, 980 (2004)
36. J.Y. Xi, X.Z. Tang, Chem. Phys. Lett. **400**, 68 (2004)
37. J.Y. Xi, X.Z. Tang, Electrochim. Acta **50**, 5293 (2005)
38. Y.W. Kim, W. Lee, B.K. Choi, Electrochim. Acta **45**, 1473 (2000)
39. D. Swierczynski, A. Zalewska, W. Wieczorek, Chem. Mater. **13**, 1560 (2001)
40. S. Kim, S.J. Park, Electrochim. Acta **54**, 3775 (2009)
41. P. Wang, S.M. Zakeeruddin, M. Gratzel, W. Kantlehner, J. Mezger, E.V. Stoyanov, O. Scherr, Appl. Phys. A Mater. **79**, 73 (2004)
42. T. Sato, G. Masuda, K. Takagi, Electrochim. Acta **53**, 4934 (2008)
43. M. Armand, F. Endres, D.R. MacFarlane, H. Ohno, B. Scrosati, Nat. Mater. **8**, 621 (2009)
44. S.H. Fang, L. Yang, J.X. Wang, H.Q. Zhang, K. Tachibana, K. Kamijima, J. Power Sources **191**, 619 (2009)
45. D.M. Li, M.Y. Wang, J.F. Wu, Q.X. Zhang, Y.H. Luo, Z.X. Yu, Q.B. Meng, Z.J. Wu, Langmuir **25**, 4808 (2009)
46. T. Welton, Chem. Rev. **99**, 2071 (1999)
47. M.M. Dharman, H.J. Choi, D.W. Kim, D.W. Park, Catal. Today **164**, 544 (2011)
48. H.L. Shim, S. Udayakumar, J.I. Yu, I. Kim, D.W. Park, Catal. Today **148**, 350 (2009)
49. S. Kim, S.J. Park, Solid State Ion. **178**, 973 (2007)